



UDC 550.42

AGE OF HYDROTHERMAL PROCESSES IN THE CENTRAL IBERIAN ZONE (SPAIN) ACCORDING TO U-Pb DATING OF CASSITERITE AND APATITE

Nailya G. RIZVANOVA¹, Sergei G. SKUBLOV¹, Ekaterina V. CHEREMAZOVA²

¹ Institute of Precambrian Geology and Geochronology of Russian Academy of Sciences, Saint Petersburg, Russia

² Mineral Exploration Network Ltd., Cardiff, United Kingdom

Results of isotope-geochemical studies by PbLS step-leaching method of cassiterite from greisens located in Logrosán granite massif (Central Iberian Zone, Spain) and apatite from hydrothermal quartz-apatite vein on its exocontact indicate that in both cases a hydrothermal event is recorded in the interval of 114-126 Ma, which has been accompanied by lead supply. Within the limits of estimation error, the same age around 120 Ma corresponds to crystallization of hydrothermal apatite, formation of sticks and micro-inclusions in cassiterite from greisens and is suggested for Au-As-Sb-Pb ore mineralization, which calls for further confirmation. Xenogenous zircon from quartz-apatite vein does not react to this relatively low-temperature hydrothermal event either with building up new generations (sticks, areas of recrystallization) or with rebalancing of U-Pb isotope system. The age of greisen formation has been confirmed to be around 305 Ma by PbLS method on final phases of cassiterite leaching. Earlier it was estimated with ⁴⁰Ar/³⁹Ar method on muscovite.

Key words: isotope geochemistry, step-leaching method, U-Pb method, Pb-Pb method, Central Iberian Zone, cassiterite, apatite

How to cite this article: Rizvanova N.G., Skublov S.G., Cheremazova E.V. Age of Hydrothermal Processes in Central Iberian Zone (Spain) According to U-Pb Dating of Cassiterite and Apatite. *Zapiski Gornogo Instituta*. 2017. Vol. 225, p. 275-283. DOI: 10.18454/PMI.2017.3.275

Introduction and problem statement. Isotope techniques play a crucial role in the research of hydrothermal processes nature, determination of ore formation age and mineral substance sources. Age determination of hydrothermal processes is based on direct dating of minerals with hydrothermal origin. As a rule, the difficulty of its realization lies in the complicated formation history of the objects under consideration, repeated activation of hydrothermal processes, frequent isolation breach in the instant isotope systems of geochronometric minerals, as well as a limited number of minerals suitable for dating. Age estimation of hydrothermal-metasomatic processes can be carried out by local U-Pb dating of zircon rims, formed in the result of these processes. For low-temperature metasomatites it is feasible to date mica and potassium feldspar with Rb-Sr method ([2] and others).

New prospects in solving the problem of dating polychronic processes appeared with the development of PbLS method – determination of isotopic age using Pb-Pb method on mineral step-leaching phases [7, 18]. The efficiency of step-leaching method has been proven for metamorphic minerals dating [1].

From the methodology position, the ore objects (Sn-W greisens and phosphate veins) mined since the Bronze Age and the territorially associated with Logrosán granite massif (Central Iberian Zone, South-Western Spain) are of special interest for hydrothermal process dating. Earlier, using U-Pb method on zircon, the crystallization age of granites has been determined as 308 ± 1 Ma [21]. Greisenization age, estimated with Ar-Ar method on muscovite from modified granites and veins with cassiterite, falls into the interval 308-313 Ma and corresponds to the age of granite intrusion [16]. Other age estimations of hydrothermal processes in this region are not available. Our attempts to determine the age of metasomatites (four samples with different mineral parageneses) with isochronal Rb-Sr and Sm-Nd methods have unfortunately failed, errorchrones obtained were characterized with very high MSWD values and inaccuracy of age estimation.

The current paper describes dating results, obtained with U-Pb and Pb-Pb step-leaching method for cassiterite from Sn-W ore veins, developing along Logrosán granites, and apatite from phos-

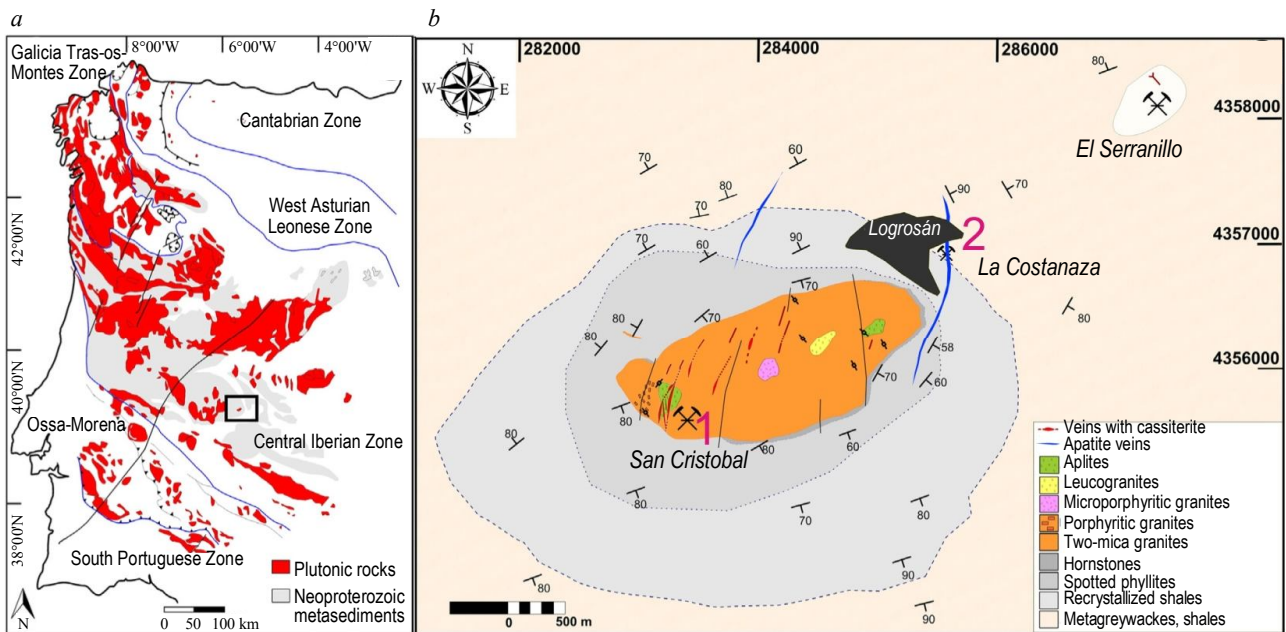


Fig. 1. Scheme of geological structure of the Central Iberian Zone (a) and Logrosán granite massif (b) according to [8]. Hammers mark sampling places from quartz-cassiterite vein in greisens (1) and quartz-apatite vein in surrounding metasediments (2)

phate veins hosted by Precambrian metasediments in the contact area of Logrosán massif. Moreover, results of local U-Pb dating are presented for zircon, derived from the phosphate vein.

Geological summary. The Logrosán granite is situated in the southern part of Sn-W metallogenic province of European Variscides (Fig.1, a). The most important characteristic of Central Iberian Zone is a wide extension of peraluminous granitoid intrusions in the latest stage of Variscan orogeny. Host rocks are presented by Neoproterozoic metasediments: metagreywackes, shales, quartzites and, to a lesser degree, metasandstones. The Logrosán intrusive (Fig.1, b), also named San Cristobal after the height it forms, is a typical small granitic cupola (around 4 km² at the surface), composed of S-type two-mica granites rich in phosphorous and fluorine. Granite intrusion resulted in metasediments contact-metamorphic changes, presented by an inner zone of hornstones and external zone of spotted phyllites and chlorite shales [10].

Intracranitic hydrothermal complex is located in the eastern part of the massif and includes Sn-(W) mineralization associated with quartz-tourmaline veins and greisenization zones of 20-50 cm in thickness and crosscutting stockworks. Hydrothermal alteration of wallrock granites is shown by muscovitization of 2-10 cm interval from the vein contact. Thickness of altered rocks increases in the stockwork zones accompanied by intensive greisenization. In general, ore mineralization comprises cassiterite (the first, oxide-silicate stage of the mineralization process) and minerals of the second sulfide stage (arsenopyrite, stannite, sphalerite, chalcopyrite etc.) with a small number of minerals from tantalite-columbite family and less common wolframite [8].

In the altered host granites cassiterite occurs as scattered hypidiomorphic crystals without inclusions of any other minerals (first generation). In quartz veins cassiterite forms zonal well-bounded bipyramidal and columnar crystals (over 5 mm) with inclusions of Nb-Ta rutile and columbite intergrowths (second generation, Fig.2, a).

Phosphate deposit La Costanaza (currently abandoned, a museum is organized on the mining site) is located in the northeastern part of Logrosán granites contact area (see Fig.1, b). The deposit consists of separate subvertical quartz-apatite veins and veinlets ranging from several centimeters to 3 m in width and served as a base for distinguishing a special «Iberian» type [10]. Most veins have a curved shape with distinctive brecciated structure (Fig.2, b). The alteration of the Schist Greywacke Complex host rocks is characterized by silification and dolomitization. Quartz often forms well-bounded druses. Apatite is mainly presented by white radial-fiber or colloform aggregate –

dahllite, or sporadically occurs as well-bounded white prismatic crystals (Fig.2, c). Accessory minerals include koalinite, calcite, Fe-Mg carbonate and Fe-Mg oxides and sulfides (arsenopyrite, chalcopyrite, pyrite, marcasite) mostly found on the periphery of quartz-apatite veins.

Hydrothermal apatite from La Costanaza deposit is defined by reduced content of Mn, Y, REE, Th, U, Pb and high content of F (3-6 wt.%) and Sr (up to 10 wt.% SrO), which makes it different from Logrosán magmatic apatite, which average SrO content does not exceed 0.01-0.12 wt.% ([10], authors' data). Elongated grains of the apatite are almost always zonal – the central part has low Sr content, whereas the outer part is rich in it, which is possibly the evidence of secondary recrystallization. The apatite from phosphorous-rich beds of host Schist Greywacke Complex (SGC) has SrO content of 0.16-0.22 wt.%, which is insignificant compared to hydrothermal apatite, whereas REE content in both magmatic and metasedimentary apatites is next higher than in the hydrothermal one [10]. Quartz-apatite veins of the deposit La Costanaza are suggested to form as a result of hydrothermal modification of sedimentary apatite from the schist and carbonate layers (source of Sr for hydrothermal apatite). In the process of long-term circulation of hydrothermal fluids Sr must have been supplied and REE subtracted.

The fluid cooling temperature after phosphate veins formation has been estimated in the interval of 125-350 °C based on fluid inclusions research in quartz; arsenopyritic geothermometer allowed to estimate the peak temperature of vein formation as 440 °C [10]. Direct dating of hydrothermal apatite by U-Pb method has never been carried out before due to extremely low U and Th content. However, with reference to a number of facts, it has been assumed that there is no genetic or temporal link between formation of phosphate veins and granite intrusion of Logrosán massif. Hydrothermal apatite has been proposed to date the Mesozoic activation period aged in the interval 201-120 Ma. In this period the Central Iberian Zone sustained a widespread formation of F-Ba polymetallic ores under similar thermal conditions [10].

Au-Sb ore occurrences are also known within Central Iberian Zone. Geochemical soil sampling carried out by the company Mineral Exploration Network Ltd. revealed contrast Sb and As anomalies, which allowed to estimate the scale of mineralization. Ore samples and placer gold grains analysis resulted in detection of galena and lead antimony sulfides (boulangerite, jamesonite), as well as inclusions of aurostibite and intergrowth of subgraphic (spongy) gold with berthierite and oxides of Sb and Pb sulphosalts. Such identifications suggest a complex paragenesis including two mineralization stages: early quartz-gold-antimonite-berthierite and late quartz-sulphosalt-aurostibite [4, 17].

Results and discussions.

Cassiterite dating. Cassiterite and rutile belong to the same mineral group – rutile group ($M^{4+}O_2$). However, unlike rutile, which has long and successfully been used as a geochronometric



Fig.2. External appearance of the rocks under investigation: a – quartz-cassiterite druse from greisens, museum exhibit from Logrosán village; b – quartz-apatite vein, under exposure and through electronic microscope; c – image from back-scattered electrons

mineral, there are only several publications dedicated to cassiterite dating, either with conventional TIMS method or with local LA-ICP-MS method (see review in [6]).

Cassiterite studies involve certain problems associated with the difficulty of its chemical decomposition during sample preparation; this is especially true in case of «young» age samples [5, 9]. Authors of the abovementioned publications preliminary washed cassiterite samples in 7M HCl solution or in 7M HCl/7M HNO₃ mixture to remove significant amounts of common lead. This procedure resulted in a substantial ²⁰⁶Pb/²⁰⁴Pb ratio increase.

It is known that most minerals appear as multiphase systems in relation to the distribution of Pb_{com} (common) and Pb_{rad} (radiogenic) in the growth zones, altered segments of a mineral caused by overlapping processes as well as a result of trapping microinclusions of minerals during crystallization. In case of cassiterite, which is highly stable towards acid effects, the question more likely refers to a presence of trace contaminations, inclusions and outgrowths of other lead-containing minerals and not to heterogeneous zones of cassiterite. As a result a different ratios of Pb_{com} and Pb_{rad} could appear for Pb component at different stages of dissolution. Therefore, to obtain additional information on Pb_{com} and Pb_{rad} distribution we have analyzed acid leaching products used for cassiterite washing.

Analytical method. Preliminary washed in the ultrasound bath cassiterite crystals from the sample S-1 (greisen vein) were thoroughly grinded. Two series of experiments were carried out involving subsequent leaching of cassiterite with different acid solutions under varying length of exposure (Table 1).

Table 1

Results of the U-Pb isotopic investigation of S-1 cassiterite

№	Treatment conditions	Isotope ratios			
		²⁰⁶ Pb/ ²⁰⁴ Pb	²⁰⁷ Pb/ ²⁰⁴ Pb	²⁰⁸ Pb/ ²⁰⁴ Pb	²³⁸ U/ ²⁰⁴ Pb
I series; 110 mg					
1	L-1, 6N HCl, 60 °C, 2 h	19.005 (0.06)	15.679 (0.09)	38.290 (0.12)	22.230 (0.37)
2	L-2, 4N HBr, 60 °C, 4 h	19.716 (0.29)	15.806 (0.17)	38.626 (0.19)	69.033 (2.64)
3	L-3, 15N HNO ₃ , 60 °C, 48 h	32.793 (1.20)	16.264 (0.92)	38.412 (0.92)	722.96 (1.98)
4	L-4, HF + HNO ₃ , 220°C, 384 h	517.37 (0.86)	41.510 (0.80)	38.422 (0.75)	n.d.
II series; 300 mg					
5	L-1, 3N HCl, 60 °C, 1 h	18.966 (0.06)	15.663 (0.09)	38.253 (0.12)	21.730 (0.60)
6	L-2, 8N HBr, 60 °C, 2 h	19.436 (0.07)	15.685 (0.09)	38.312 (0.12)	37.810 (0.35)
7	L-3, 15N HNO ₃ , 220 °C, 16 h	25.941 (0.20)	16.016 (0.12)	38.373 (0.14)	275.90 (0.63)
8	L-4, 10N HCl, 220 °C, 256 h	286.33 (0.78)	16.264 (0.92)	39.948 (0.34)	4997.5 (0.85)
9	L-5, HF + HNO ₃ , 220 °C, 528 h	855.40 (0.55)	59.466 (0.49)	39.844 (0.42)	16709 (0.56)

Note. Isotope ratios corrected for blank and fractionation. Numbers in brackets correspond to the measurement error ($\pm 2\sigma$) in percent.

After each acidic treatment solutions were collected into boxes, evaporated and converted in to bromide form. The residues were twice rinsed with water, dried out and used for the next acidic treatment.

The subsequent treatments series of cassiterite portions did not lead to a full decomposition of the sample. All the leaching products were used to determine isotope composition of lead and after introducing a mixed indicator ²⁰⁸Pb-²³⁵U – to estimate lead and uranium content. Pb and U separation from cassiterite was carried out on ion-exchange resin in HBr form using method [14] with subsequent U detachment on UTEVA resin. The experimental blank did not exceed 0.05 ng of Pb.

Isotope ratios of lead and uranium were measured with a multicollector mass spectrometer TRITON TI in the Laboratory of Geochronology and Geochemistry of Isotopes, Institute of Precambrian Geology and Geochronology, Russian Academy of Sciences. Calculations of isotope ra-

tios and U-Pb age of cassiterite were performed with a standard procedure of Pb/U ratios (2σ) measurement error using K. Ludwig's computer programs [12, 13]. It should be noted that the use of leaching products for U-Pb system examination could be legitimate only if the dissolution is congruent and there is no fractionation of lead and uranium.

Results. The first three leaching phases in the first and second experiment series have low $^{206}\text{Pb}/^{204}\text{Pb}$ ratio (in the interval 19.0-32.8, Table 1). Calculations and formulations were carried out in $^{235}\text{U}/^{204}\text{Pb} - ^{206}\text{Pb}/^{204}\text{Pb}$ coordinates. When using calculation data for leaching products 1, 2, 3, 5 and 6 the imaging points shape an errorchrone with the following parameters: age 126 ± 5 Ma, MSWD = 179 (Fig.3, a). Adding data on leaching product 7 increases error of age determination (129 ± 24 Ma) and MSWD = 752, although the age interval stays the same.

Subsequent acidic treatment of cassiterite allowed to obtain leaching products with higher content of radiogenic lead ($^{206}\text{Pb}/^{204}\text{Pb}$ ratio falls into the interval 286-855). Using data from three leaching products 7, 8 and 9 (Table 1), an isochrone with the age 303 ± 3 Ma has been plotted in $^{206}\text{Pb}/^{204}\text{Pb} - ^{207}\text{Pb}/^{204}\text{Pb}$ coordinates (MSWD = 1.8, Fig.3, b). Inclusion of leaching product 4 increases the age determination error (298 ± 47 Ma, MSWD = 3.8). High mean MSWD confirms that cassiterite contains at least two radiogenic Pb components of different ages.

Thus, as a result of subsequent series of acidic cassiterite leaching, two age values have been obtained. The age 303 ± 3 Ma can be attributed to cassiterite formation. It agrees with the age of magmatic zircon from Logrosán granite massif – 308 ± 1 Ma [10] – and with $^{40}\text{Ar}/^{39}\text{Ar}$ age from 308 to 303 Ma estimated for muscovite from Sn-W ore-bearing veins crosscutting the granites, which contain the analyzed cassiterite [16].

Apparently, as a result of cassiterite leaching at the first three stages of acidic treatment (Table 1), external sticks and microinclusions of other mineral phases containing significant amounts of common lead were being removed. This brought lead can be attributed to the second (later) stage of hydrothermal activity with the age of 201-120 Ma associated with an early Jurassic rifting and tholeiitic magmatism, which caused widespread formation of F-Ba-Pb-Zn ore veins within Central Iberian Zone [10]. The age of 126 ± 5 Ma determined for cassiterite using the first leaching products falls into the mentioned time interval.

Apatite dating. The sample of apatite monofraction (P-1) was collected from a new-made shearing cut in the main quartz-apatite vein of La Costanaza deposit crosscutting Neoproterozoic metasediments. According to classification of hydrothermal apatite proposed in [10] the apatite under consideration belongs to the fibrous type.

Analytical method. The apatite derived from the sample P-1 was additionally cleaned under binocular microscope for isotope research. To collect grains absolutely free from inclusions appeared to be impossible. Pb and U isotope analysis of the bulk portion of apatite 1 (Table 2) demonstrated the high content of common lead ($^{206}\text{Pb}/^{204}\text{Pb} = 20.7$). A decision was made to apply step-leaching in order to extract Pb with different ratios of Pb_{com} and Pb_{rad} components. For this purpose

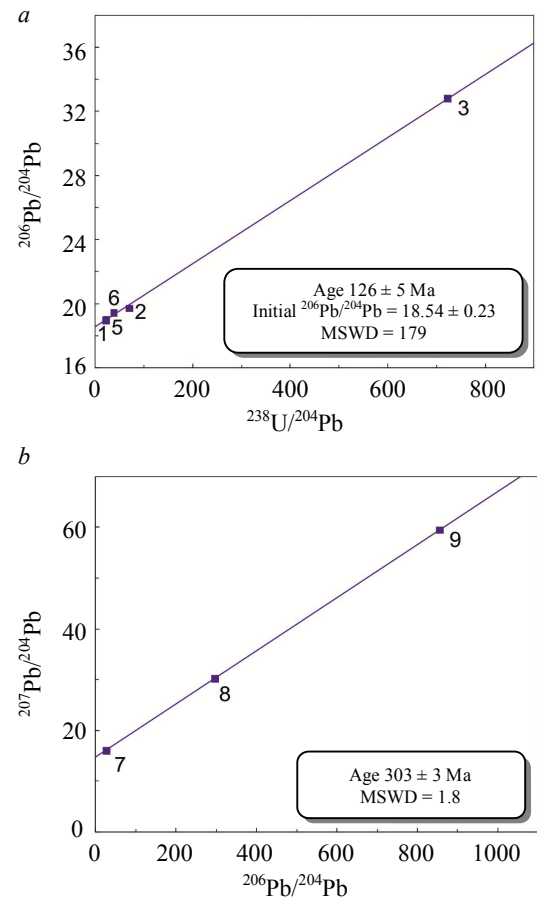


Fig.3. Results of isotope-geochemical study of cassiterite (S-1): a – plot in $^{238}\text{U}/^{204}\text{Pb} - ^{206}\text{Pb}/^{204}\text{Pb}$ coordinates, first leaching products; b – plot in $^{206}\text{Pb}/^{204}\text{Pb} - ^{207}\text{Pb}/^{204}\text{Pb}$ coordinates, subsequent leaching products. The size of dots bears no correspondence to measurement errors

a new portion of apatite (I series; 90 mg) was treated with 3N HCl twice, 1 h each time at the temperature 20 °C. The first leaching product was not measured. Isotope analysis was performed for the second one. The third portion of apatite (II series; 143 mg) was thoroughly leached at 20 °C in 1.5N HCl during 2 h (leaching product 3) and 1 h (leaching product 4). It should be noted that in all series of experiments multistep leaching failed to fully dissolve the apatite portion, which points to its modified structure and presence of trace microinclusions. Microprobe analysis of the non-dissolved residue showed that it consists of quartz and individual grains of goyazite (aluminophosphate of strontium).

Table 2

Results of the U-Pb isotopic investigation of P-1 apatite

№	Treatment conditions	Isotope ratios					206Pb/238U age, Ma
		206Pb/204Pb ^a	207Pb/204Pb ^a	208Pb/204Pb ^a	238U/204Pb ^b	206Pb/238U ^b	
1	Bulk apatite	20.696 (0.46)	15.775 (0.17)	39.523 (0.24)	59.480 (3.50)	0.01719 (6.70)	109.2 ± 6.8
I series; 90 mg							
2	3N HCl, 20 °C, 1 h	19.832 (0.22)	15.740 (0.13)	39.141 (0.17)	8.916 (4.12)	0.01779 (26.6)	108.7 ± 28
II series; 143 mg							
3	1.5N HCl, 20 °C, 2 h	20.656 (0.36)	15.764 (0.32)	39.373 (0.33)	52.466 (1.44)	0.01874 (6.80)	118.8 ± 6.8
4	1.5N HCl, 20 °C, 1 h	20.324 (0.36)	15.790 (0.20)	39.229 (0.24)	35.034 (2.70)	0.01857 (9.25)	117.3 ± 9.4
5	Plagioclase	19.697 (0.54)	15.217 (0.02)	–	–	–	–

Note: a – isotope ratios corrected for laboratory blank and fractionation; b – isotope ratios corrected for blank, fractionation and common Pb.

Results. The obtained results for apatite selected in I and II experimental series are presented in Table 2. There has not been registered any significant difference in $^{207}\text{Pb}/^{204}\text{Pb}$ and $^{206}\text{Pb}/^{204}\text{Pb}$ ratios in leaching products, thus a plot has been constructed in $^{238}\text{U}/^{204}\text{Pb} - ^{206}\text{Pb}/^{204}\text{Pb}$ coordinates (Fig.4). For four points (bulk apatite and three leaching products, Table 2) the age was estimated to be 114 ± 8 Ma (MSWD = 1.9). High mean MSWD indicates that bulk apatite is quite heterogeneous and may contain inherited components. The initial ratio of $^{206}\text{Pb}/^{204}\text{Pb}$ obtained from age determination equals 19.680 ± 0.049 . Analysis has also been undertaken for plagioclase derived from the apatite vein sample – its isotope ratio is 19.697. Adjustment for initial lead content allowed to calculate apatite age using $^{206}\text{Pb}/^{238}\text{U}$ ratio, the mean value of which across four points amounted to 114 Ma (Table 2). The age calculated in Tera-Wasserburg coordinates equals 111 ± 12 Ma (MSWD = 0.023).

Obtained results can be considered preliminary. A more ideal extraction of apatite monofraction and implementation of suggested dating approach by using subsequent series of leaching could significantly clarify development history of quartz-apatite veins. Nevertheless, a hypothesis on Mesozoic (201-120 Ma) age of hydrothermal phosphate vein genesis isolated in time from the age of Logrosán granites formation, which was proposed in publication [10] according to several indirect indicators, has been independently supported by PbLS dating method.

Zircon dating. Around 25 grains and grain fragments were derived from a quartz-apatite vein (sample P-1). 15 of them were large enough for dating purposes.

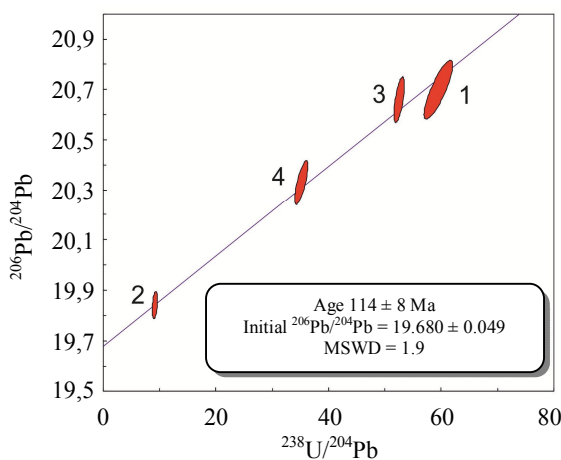


Fig.4. Results of isotope-geochemical study of apatite (P-1) in $^{238}\text{U}/^{204}\text{Pb} - ^{206}\text{Pb}/^{204}\text{Pb}$ coordinates. Ellipses of measurement errors correspond to 2σ , including inaccuracy of decay constant

Analytical method. Zircon dating with U-Pb method was carried out in the Center of Isotope Research, Russian Geological Research Institute, on the ion microprobe SHRIMP-II with standard technique [20]. Points for analysis were chosen using images of zircon grains in transmitted light, in cathodoluminescence (CL) and backscattered electrons mode. Content of REE and rare elements in zircon was estimated for the points earlier dated with U-Pb method (16 points) on the ion microprobe Cameca IMS-4f in Yaroslavl Branch of the Institute of Physics and Technology with methods described in [3, 11]. The size of analyzed mineral area did not exceed 15-20 μm in diameter; relative measurement error for most tests was 10-15 %; element detection threshold on the average amounted to 10 ppb. To plot spectra of REE distribution, zircon composition was normalized to the chondrite CI [15]. Estimation of crystallization temperature was carried out with Ti thermometer in zircon [19].

Results. Zircon grains are mostly short-columnar, with long axis size of maximum 100 μm . In CL they are characterized by a distinct oscillatory growth zoning in dark grey shades, less frequently – by sectorial zoning. No clearly defined rims or zones of zircon recrystallization have been identified.

In Tera-Wasserburg concordia diagram imaging points for zircon derived from quartz-apatite vein sample P-1 correspond to individual values of $^{238}\text{U}/^{206}\text{Pb}$ age that fall into the interval between 550 to 915 Ma (Fig.5, a). One point has an age over 2016 Ma. The diagram of relative $^{238}\text{U}/^{206}\text{Pb}$ age distribution in zircon has a distinct peak around 610 Ma (Fig.5, b). Using five points attributed to this peak, concordant age of 606 ± 7 Ma has been calculated.

Earlier in [21] local dating of zircon from Logrosán granite massif has been carried out using LA-ICP-MS method and resulted in following – for 40 % of grains U-Pb age estimations were older than it could be expected for Variscan granites. For the major part of xenogenous zircon apparently captured from metasedimentary complex, which has been cut through by the granites, estimated age falls into the interval 550-847 Ma. Paleoproterozoic age has been identified for individual grains [21].

Comparison of age distribution spectra for zircon captured by Logrosán granites and zircon from Neoproterozoic metasedimentary Schist Greywacke Complex (according to multiple literature sources) showed high degree of their conformity. Notably, in metasediments clearly prevails zircon aged around 600 Ma (Fig.10 in [21]). Apparently, dated zircon from the phosphate vein has all been

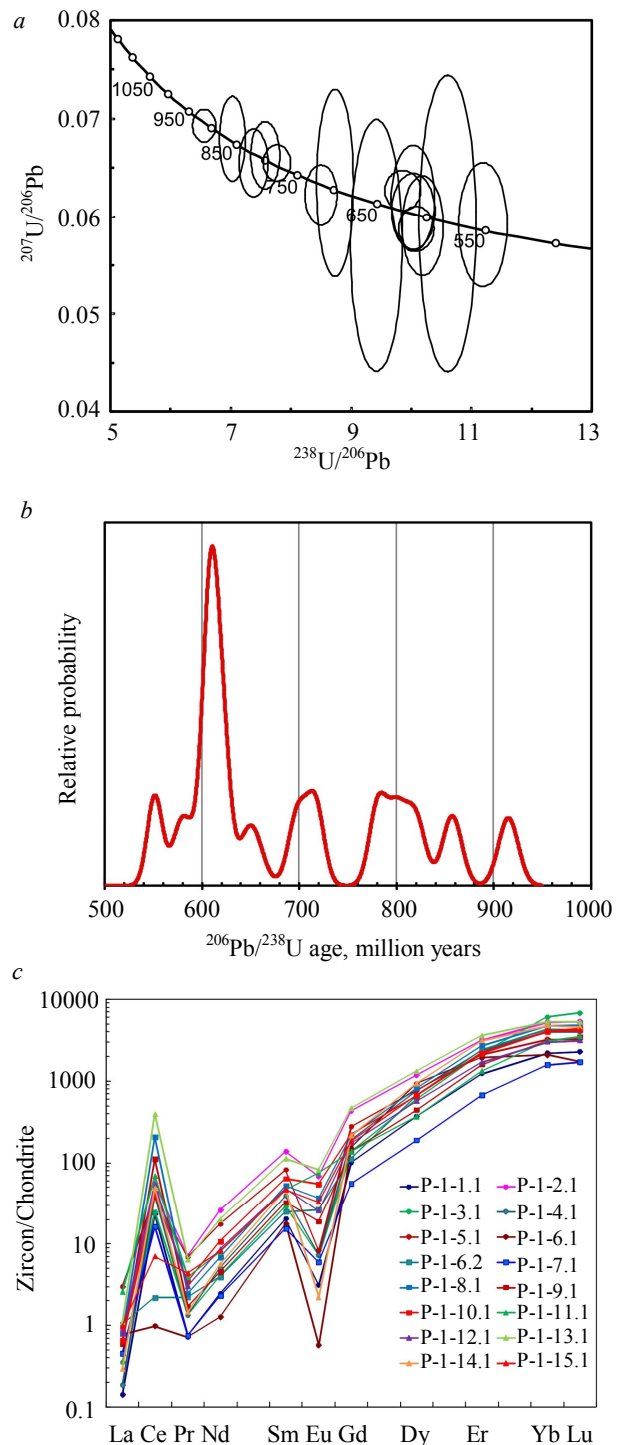


Fig.5. Results of isotope-geochemical study of zircon (P-1):
a – Tera-Wasserburg concordia diagram;
b – probability diagram for $^{206}\text{Pb}/^{238}\text{U}$ age;
c – spectra of REE distribution in zircon



captured from surrounding rocks of SGC. Thermal event aged around 308 Ma (granite intrusion) and subsequent hydrothermal processes registered with PbLS method had no influence upon U-Pb isotope system of xenogenous Neoproterozoic zircon derived from quartz-apatite vein.

The character of REE distribution in zircon corresponds to its detritus nature. REE distribution spectra are highly differentiated with an increase from light to heavy REE with an overall REE content around 1300 ppm, there are clearly defined positive Ce-anomaly and negative Eu-anomaly (Fig.5, c). Hf content in zircon averages approximately 9000 ppm, Y – 2000 ppm, P – 400 ppm, Li – 17 ppm. Temperature of zircon crystallization calculated with Ti thermometer [19] on the average equals 740 °C. Such peculiarities of zircon composition from the viewpoint of rare elements clearly point to its crustal origin from acid magmatic melts. Geochemical characteristics do not contain any traces of hydrothermal processes associated with phosphate vein formation.

Conclusions. Therefore, the results of isotope-geochemical studies of cassiterite from greisens located in Logrosán granite massif (Central Iberian Zone, Spain) and apatite from hydrothermal quartz-apatite vein on its exocontact using PbLS step-leaching method indicate that in both cases in the interval of 114-126 Ma a hydrothermal event is recorded, which has been accompanied by lead supply. Within the limits of estimation error, the same age around 120 Ma corresponds to crystallization of hydrothermal apatite, formation of sticks and micro-inclusions in cassiterite from greisens and is suggested for Au-As-Sb-Pb ore mineralization, which calls for further confirmation. Xenogenous zircon from quartz-apatite vein does not react to this relatively low-temperature hydrothermal event either with building up new generations (sticks, areas of recrystallization) or with rebalancing of U-Pb isotope system. The age of greisen formation has been confirmed to be around 305 Ma by PbLS method on final phases of cassiterite leaching. Earlier it was estimated with $^{40}\text{Ar}/^{39}\text{Ar}$ method on muscovite. [16].

Acknowledgements. Authors thank O.L.Galankina, E.S.Bogomolov (Institute of Precambrian Geology and Geochronology of Russian Academy of Sciences), S.G.Simakin, E.V.Potapov (Yaroslavl Branch of the Institute of Physics and Technology) and colleagues from the Center of Isotope Research, Russian Geological Research Institute for undertaken analytical studies. This research has been carried out with financial support from the Ministry of Education and Science of Russian Federation as a basic design part of the state assignment in the field of science N 5.9248.2017/VU for the period 2017-2019.

REFERENCES

1. Levchenkov O.A., Rizvanova N.G., Makeev A.F. et al. Capabilities and Constraints of the Pb-Pb Dating of Metamorphogenic Minerals Using the Step-Leaching Method. *Geohimija*. 2009. N 11, p. 1123-1137 (in Russian).
2. Chernyshev I.V., Kovalenker V.A., Gol'cman Ju.V. et al. Isochron Rb-Sr Dating of Late Paleozoic Epithermal Mineralization Processes on the Example of Kayragach Gold Deposit (Kurama Ore District, Middle Tian Shan). *Geohimija*. 2011. N 2, p. 115-128 (in Russian).
3. Fedotova A.A., Bibikova E.V., Simakin S.G. Zircon Geochemistry (Ion Microprobe Data) as an Indicator of Mineral Genesis in Geochronological Research. *Geohimija*. 2008. N 9, p. 980-997 (in Russian).
4. Cheremazova E.V., Novoselov K.A., Svetlova Ju.L. Mineralogical and Geochemical Characteristics of Au-Sb Mineralization on Agujoncillo Site (Extremadura, Spain). *Regional'naja geologija i metallogenija*. 2016. N 68, p. 100-107 (in Russian).
5. Yuan S., Peng J., Hu R. et al. A Precise U-Pb Age on Cassiterite from the Xianghualing Tin-Polymetallic Deposit (Hunan, South China). *Mineralium Deposita*. 2008. Vol. 43, p. 375-382.
6. Chen X.-C., Hu R.-Z., Bi X.-W. et al. Cassiterite LA-MC-ICP-MS U/Pb and Muscovite $^{40}\text{Ar}/^{39}\text{Ar}$ Dating of Tin Deposits in the Tengchong-Lianghe Tin District, NW Yunnan, China. *Mineralium Deposita*. 2014. Vol. 49, p. 843-860.
7. Frei R., Kamber B.S. Single mineral Pb-Pb dating. *Earth and Planetary Science Letters*. 1995. Vol. 129, p. 261-268.
8. Chicharro E., Martin-Crespo T., Gomez-Ortiz D. et al. Geology and Gravity Modeling of the Logrosán Sn-(W) Ore Deposits (Central Iberian Zone, Spain). *Ore Geology Reviews*. 2015. Vol. 65, p. 294-307.
9. Gulson B.L., Jones M.T. Cassiterite: Potential for Direct Dating of Mineral Deposits and a Precise Age for the Bushveld Complex Granites. *Geology*. 1992. Vol. 20, p. 355-358.
10. Vindel E., Chicharro E., Villaseca C. et al. Hydrothermal Phosphate Vein-Type Ores from the Southern Central Iberian Zone, Spain: Evidence for their Relationship to Granites and Neoproterozoic Metasedimentary Rocks. *Ore Geology Reviews*. 2014. Vol. 62, p. 143-155.



11. Hinton R.W., Upton B.G.J. The Chemistry of Zircon: Variations Within and Between Large Crystals from Syenite and Alkali Basalt Xenoliths. *Geochimica et Cosmochimica Acta*. 1991. Vol. 55, p. 3287-3302.
12. Ludwig K.R. PbDat 1.21 for MS-dos: A Computer Program for IBM-PC Compatibles for Processing Raw PbU-Th Isotope data. Version 1.07. U.S. Geological Survey, Open-File Report 88-542, 1991, p. 35.
13. Ludwig K.R. Isoplot/Ex 3. A Geochronological Toolkit for Microsoft Excel. Berkeley Geochronology Center. Special publication N 4. 2003, p. 74.
14. Manhès G., Minster J.E., Allegre C.J. Comparative Uranium-Thorium-Lead and Rubidium-Strontium Study of the Severin Amphoterite: Consequences for Early Solar System Chronology. *Earth and Planetary Science Letters*. 1978. Vol. 39, p. 14-24.
15. McDonough W.F., Sun S.S. The Composition of the Earth. *Chemical Geology*. 1995. Vol. 120, p. 223-253.
16. Chicharro E., Boiron M.-C., Lopez-García J.A. et al. Origin, Ore Forming Fluid Evolution and Timing of the Logrosan Sn-(W) Ore Deposits (Central Iberian Zone, Spain). *Ore Geology Reviews*. 2016. Vol. 72, p. 896-913.
17. Cheremazova E., Skublov S., Novoselov K. et al. Primary Au Prospecting Results in the Logrosán Area (Central Iberian Zone, Spain). *Journal of Iberian Geology*. 2015. Vol. 41, p. 223-232.
18. Frei R., Kramers J.D., Przybyłowicz W.J. et al. Single Mineral Dating by the Pb-Pb Step-Leaching Method: Assessing the Mechanisms. *Geochimica et Cosmochimica Acta*. 1997. Vol. 61, p. 393-414.
19. Watson E.B., Wark D.A., Thomas J.B. Crystallization Thermometers for Zircon and Rutile. *Contributions to Mineralogy and Petrology*. 2006. Vol. 151, p. 413-433.
20. Williams I.S. U-Th-Pb Geochronology by Ion Microprobe. *Reviews in Economic Geology*. 1998. Vol. 7, p. 1-35.
21. Chicharro E., Villaseca C., Valverde-Vaquero P. et al. Zircon U-Pb and Hf Isotopic Constraints on the Genesis of a Post-Kinematic S-type Variscan Tin Granite: the Logrosan Cupola (Central Iberian Zone). *Journal of Iberian Geology*. 2014. Vol. 40, p.451-470.

Authors: **Nailya G. Rizvanova**, Candidate of Geological & Mineral Sciences, Senior Researcher, rizng@mail.ru (Institute of Precambrian Geology and Geochronology of Russian Academy of Sciences, Saint Petersburg, Russia), **Sergei G. Skublov**, Doctor of Geological & Mineral Sciences, Leading Researcher, skublov@yandex.ru (Institute of Precambrian Geology and Geochronology of Russian Academy of Sciences, Saint Petersburg, Russia), **Ekaterina V. Cheremazova**, Geologist, kate@kareliangold.com (Mineral Exploration Network Ltd., Cardiff, United Kingdom).

The paper was accepted for publication on 14 February, 2017.